Overview on Current Modelling Strategies of Point Clouds for Deformation Analysis

Überblick aktueller Methoden zur Modellierung von Punktwolken für die Deformationsanalyse

Hans Neuner, Christoph Holst, Heiner Kuhlmann

Terrestrial laser scanning was used for deformation monitoring of structures and geoscientific objects already at an early stage of its employment for engineering geodetic tasks. This paper gives an overview on current state of the art methods and fields of applications concerning the modelling of point clouds obtained with this measuring technology, by following two aims. On the one hand, the presentation of modelling methods used for retrieving deformation information additional to the ones given in /Bureick et al. 2016/ and /Wunderlich et al. 2016/ of this special issue, is intended. On the other hand, a structuring of the modelling methods with regard to the most common types of analysed measuring objects in engineering geodesy is performed. The aim of this structuring is to create a conceptual link between the model category according to /Ohlmann-Lauber & Schäfer 2011/, the adopted modelling strategy and the object type.

Keywords: Point cloud modelling, deformation analysis, 2nd order surfaces, radial basis function

Bereits frühzeitige Einsätze des terrestrischen Laserscannings für ingenieurgeodätische Aufgaben haben die Überwachung baulicher Strukturen und geowissenschaftlicher Messobjekte zum Inhalt. Dieser Überblicksartikel beschäftigt sich mit aktuellen Methoden und Anwendungsbereichen der Modellierung von Punktwolken aus terrestrischen Laserscans. Zwei Ziele werden dabei verfolgt: Einerseits werden zu den Beiträgen von /Bureick et al. 2016/ und /Wunderlich et al. 2016/ in diesem Schwerpunktheft ergänzende Modellierungsmethoden zur Herleitung der Deformationsinformation vorgestellt. Das zweite Ziel ist die Strukturierung der Modellierungsmethoden in Bezug zu häufig untersuchten Typen von Messobjekten. Damit soll eine thematische Verbindung zwischen den von /Ohlmann-Lauber & Schäfer 2011/ etablierten Modelltypen zur Ableitung von Deformationen, den Modellierungsmethoden und dem Typus des Messobjekts entstehen.

Schlüsselwörter: *Modellierung von Punktwolken, Deformationsanalyse, Flächen 2. Ordnung, radiale Basisfunktionen*

1 INTRODUCTION

Acquired point clouds are modelled for different purposes: The object's computational visualization from different perspectives, the generation of terrain and building models for the purpose of planning activities, the presentation of construction elements in information systems like Building Information Modelling (BIM) and the task of reverse engineering to determine discrepancies of a fabricated system component to its CAD plan are only some examples. Each of these examples is a core task in at least one discipline. As a consequence, the modelling tasks deal with objects of different spatial dimensions and have different requirements regarding the accuracy. This contribution focuses exclusively on tasks dealing with the modelling of point clouds to determine deformations and having

a distinctive engineering geodetic character according to /Kuhlmann et al. 2014/. In accordance with this objective, the modelled point clouds mainly originate from terrestrial laser scanners (TLS).

Since the advent of the terrestrial laser scanner in engineering geodesy, it has been used to detect geometric changes of measured objects. The missing reproducibility of the measured points impedes an immediate derivation of deformations, even if a geometric comparative basis between the point clouds of different epochs is established. For this reason, the allocation of identical elements of the measured objects in different point clouds has to be realized in a separate step which usually implies a geometric modelling of the point cloud. In recent years, a variety of modelling methods has been developed and proved. /Ohlmann-Lauber & Schäfer 2011/ established an initial systematization of these methods by pointing up five categories which are characterized by the geometric quantity used to determine the deformations:

- Point based models: single points;
- Point cloud based models: point clouds;
- Surface based models: grid structures;
- Geometry based models: continuous surfaces;
- Parameter based models: parameters of approximating surfaces.

Point based models are applied solely in case of repeated TLS-measurements from a fixed viewpoint. This approach is based on the comparison of measurements in the same spatial direction. In point cloud based models, relationships between point clouds are established by means of point-orientated algorithms based on transformation instructions like the Iterative-Closest-Point algorithm (ICP). In the surface based approach, the point clouds are modelled by building a surface consisting of point grids. The respective points are either measured directly (e. g. triangle mesh) or they are interpolated (e. g. octrees). The geometry based and the parameter based methods both use geometric forms to represent the surface. The approaches differ in their derivation of the deformations: The geometry based models aim to describe rigid body movements by indicating the estimated surface's change in position and orientation. In contrast, the parameter based approach can be seen as an extension of the former method, as also deformations are revealed by statistically testing the change of characteristic surface parameters. As can be seen, only the three last-mentioned categories are based on a modelling of the point clouds. For this reason, only issues being relevant for one of these categories are addressed in the following.

The purpose of this contribution is twofold: On the one hand, an overview of research activities dealing with the modelling of point clouds with regard to the derivation of deformations is provided. This overview is subdivided according to the measured objects and conveys an application-orientated state of the art of the areal deformation analysis of these objects. On the other hand, the methods used for these tasks are presented and systematized with regard to their present field of application. Selected methods such as the modelling with geometric free-form elements are treated separately in /Bureick et al. 2016/ and /Wunderlich et al. 2016/ in this special issue.

The paper is structured as follows: *Section 2* deals with the mathematical principles of the methods mentioned in the overview of the research activities. The measuring-object-related synthesis of the state of the art is given in the third section. Research activities are cited as representatives for the application of a respective method with regard to the deformation analysis in connection with a respective object. The fourth section concludes the contents of the contribution.

2 METHODOLOGICAL FUNDAMENTALS

2.1 Modelling with 2nd order surfaces

The general equation of a 2nd order surface can be written as follows /Bronstein et al. 2001/:

$$a_{11}x^2 + a_{22}y^2 + a_{33}z^2 + 2a_{12}xy + 2a_{23}yz + 2a_{31}zx + 2a_{14}x + 2a_{24}y + 2a_{34}z + a_{44} = 0. \quad (1)$$

Therein (x, y, z) are the coordinates of a point on the surface and a_{ij} ($i = 1, \ldots, 4$ and $j = 1, \ldots, 4$) are the surface parameters to be estimated. Eq. (*1*) is a constraint for each measured point of a point cloud. All constraints summarised and extended by appropriate residual terms, in order to avoid inconsistencies, build the functional part of a Gauss-Helmert adjustment model to estimate the ten parameters a_{ij}. The covariance matrix of the coordinates represents the stochastic model. A feasible approach for setting up this matrix can be found in /Kauker et al. 2016/ of the first avn-special issue on this topic. Due to the homogeneity of Eq. (*1*), a unique estimation of the parameters different to the trivial solution is only possible, if an additional restriction according to a part of the unknown coefficients of the adjustment is introduced. /Drixler 1993/ proposes the following restriction:

$$a_{11}^2 + a_{22}^2 + a_{33}^2 + 2a_{12}^2 + 2a_{23}^2 + 2a_{31}^2 = 1 \quad (2)$$

due to its translational and rotational invariance. Thus, the adjustment can be solved on basis of the known Gauss-Helmert model. The linearisation of Eq. (*1*) with respect to the measurements as well as the linearisation of the constraint (*2*) with respect to the unknowns requires appropriate approximate values of the parameters. An approach to circumvent this requirement is shown by /Drixler 1993/; he transfers the Gauss-Helmert model in a Gauss-Markov model and discard the coefficients a_{i4} by Gaussian elimination. The first six surface parameters can be estimated as the eigenvector belonging to the smallest eigenvalue of the spectral decomposition of a quadratic form, which is similar to the normal equation system. The discarded a_{i4} surface parameters result from a back substitution and depend on the already estimated parameters.

Subsequently, the shape of the surface can be determined automatically based on the sign of the invariants of a 2nd order surface. The surface invariants are obtained for $a_{ij} = a_{ji}$ as follows:

$$\Delta = \det\begin{pmatrix} a_{11} & a_{12} & a_{13} & a_{14} \\ a_{21} & a_{22} & a_{23} & a_{24} \\ a_{31} & a_{32} & a_{33} & a_{34} \\ a_{41} & a_{42} & a_{43} & a_{44} \end{pmatrix}; \; \delta = \det\begin{pmatrix} a_{11} & a_{12} & a_{13} \\ a_{21} & a_{22} & a_{23} \\ a_{31} & a_{32} & a_{33} \end{pmatrix};$$

$$S = a_{11} + a_{22} + a_{33};$$

$$T = a_{22}a_{33} + a_{33}a_{11} + a_{11}a_{22} - a_{23}^2 - a_{31}^2 - a_{12}^2. \quad (3)$$

	$\delta \neq 0$		$\delta = 0$
	$S\,\delta > 0$ and $T > 0$	$S\,\delta$ and T not both > 0	
$\Delta < 0$	Ellipsoid	Hyperboloid of two sheets	Elliptical Paraboloid
$\Delta > 0$	Imaginary Ellipsoid	Hyperboloid of one sheet	Hyperbolical Paraboloid
$\Delta = 0$	Imaginary Cone	Cone	Cylinder: $T > 0$: imaginary elliptic $T < 0$: hyperbolic $T = 0$: parabolic

Tab. 1 | Types of the 2nd order surfaces in dependence of the invariants sign according to Eq. (*3*)

One obtains the decision tree restricted to curved surfaces, shown in *Tab. 1*.

By nature, imaginary surfaces do not play a role and therefore, they are highlighted grey in the table. The inequalities and equalities from *Tab. 1* are formulated in a strict mathematical-geometric sense. In consequence of the estimation of the surface parameters, the fulfilment of the conditions given in *Tab. 1* needs to be proven statistically. /Hesse & Kutterer 2006/ proposed a test procedure based on /Kutterer & Schön 1999/ and /Schön & Kutterer 1999/. In a multidimensional test significant deviations from zero of all invariants will be proven and if the test fails, each invariant will be evaluated in a single test. A Monte-Carlo simulation based on a multi variate normal distribution, which is centred in the surface parameters, is an alternative opportunity. A result obtained with this approach for the classification of a (simulated) ellipsoid in dependence of the noise level is shown in *Fig. 2*.

Exemplary for the method outlined in this section, the approximation of the dam's surface by a 2nd order surface and the subsequent classification as ellipsoid are presented in *Fig. 1*.

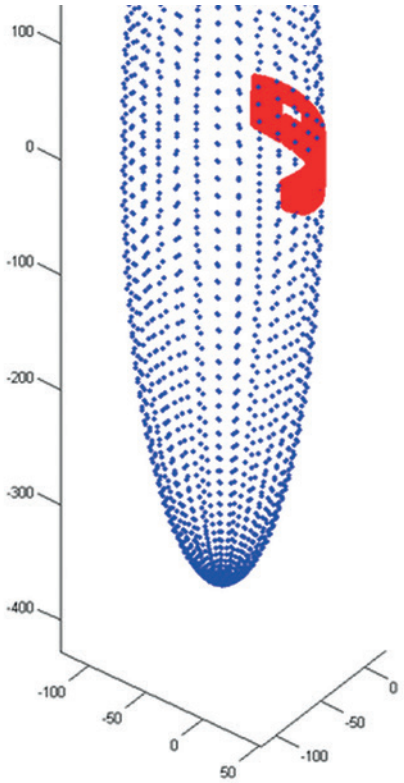

Fig. 1 | Automatic detection of the dam's surface as Ellipsoid /Eling & Kutterer 2007/

2.2 Modelling with radial basis functions

This type of modelling belongs to strategies which use a combination of functions of the same type, the so-called basis functions, to represent the surface (e. g., /Carr et al. 2001/). The procedure is similar for example to the frequency analysis of a time series in which this is represented as a sum of sine and cosine functions of varying arguments in terms of the Fourier theory, or to empirical density modelling by kernel density estimation. This approximation method is particularly suitable for tasks with irregularly distributed points on the surface, as it is the case in TLS. The radial functions used for the approximation are real functions of the directional distance between a location $\boldsymbol{x}$ and a centre point $\boldsymbol{c}$, defined in the range [0, ∞) and usually unlimited:

$$\varphi(\boldsymbol{x}) = \varphi(\|\boldsymbol{x} - \boldsymbol{c}\|) \,. \tag{4}$$

In (*4*), $\|\cdot\|$ denotes the norm operator, which is usually the Euclidean norm. In literature (e. g. /Carr et al. 2001/) there are numerous radial functions, the most common ones are summarized in *Tab 2*.

Gauss	$\varphi(r) = \exp(-mr^2)$
Multiquadric	$\varphi(r) = \sqrt{r^2 + m^2}$
Biharmonic	$\varphi(r) = r$
Triharmonic	$\varphi(r) = r^3$
Thin plate spline	$\varphi(r) = r^2 \log r$

Tab. 2 | Commonly used radial functions

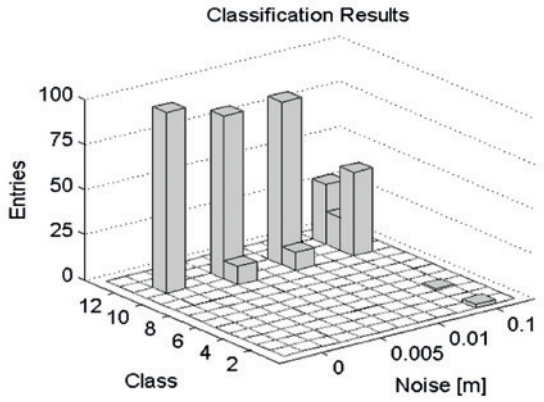

Fig. 2 | Result of a Monte-Carlo-Simulation for the classification of an Ellipsoid: Class 10: Ellipsoid of rotation; Class 11: Ellipsoid; Class 12: Hyperboloid of two sheets /Hesse & Kutterer 2006/

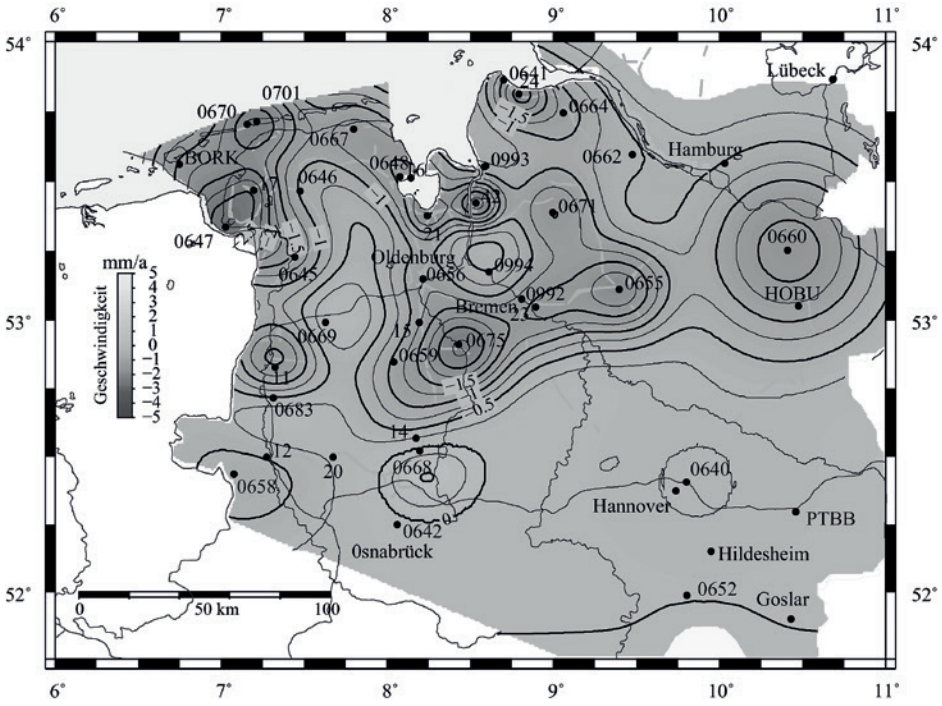

Fig. 3 | Field of vertical velocities of Northern Germany modelled with radial basis functions /IKÜS 2008/

The functions in *Tab. 2* are specified in dependence of the radius $r = \boldsymbol{x} - \boldsymbol{c}$. Some functions include further parameters (designated by m in *Tab. 2*) in addition to the radius, which affect their shape (e. g. the extent of the Gaussian).

The starting point for the representation of a surface by radial basis functions is the interpolation of N discrete points $\boldsymbol{x}_i$, $i = 1, \ldots, N$, by a smooth surface s. If smoothness is expressed as

$$\int_{\mathbb{R}^3} \left(\frac{\partial^2 s}{\partial x^2}\right)^2 + \left(\frac{\partial^2 s}{\partial y^2}\right)^2 + \left(\frac{\partial^2 s}{\partial z^2}\right)^2 + 2\left(\frac{\partial^2 s}{\partial x \partial y}\right)^2 + 2\left(\frac{\partial^2 s}{\partial y \partial z}\right)^2 + 2\left(\frac{\partial^2 s}{\partial z \partial x}\right)^2 d\boldsymbol{x}, \tag{5}$$

then it can be shown that surfaces of the form

$$s(\boldsymbol{x}) = p(\boldsymbol{x}) + \sum_{i=1}^{N} \lambda_i \|\boldsymbol{x} - \boldsymbol{x}_i\| \tag{6}$$

are of maximum smoothness. Therein $p(\boldsymbol{x})$ denotes a linear polynomial, λ_i real numbers, and $\|\boldsymbol{x} - \boldsymbol{x}_i\|$ the Euclidean norm. Eq. (*6*) is a special case of the representation of a surface by radial basis functions:

$$s(\boldsymbol{x}) = p(\boldsymbol{x}) + \sum_{i=1}^{N} \lambda_i \varphi(\|\boldsymbol{x} - \boldsymbol{c}_i\|). \tag{7}$$

From the equivalence of the Eq. (*4*) and (*7*) it becomes obvious that the centre points $\boldsymbol{c}_i$ correspond to the measuring points $\boldsymbol{x}_i$. The approximation is done by estimating the weights λ_i, $i < N$, which control the contribution of each radial basis function to an estimated point of the surface. From the structure of Eq. (*7*) it can be seen, that the Gauss-Markov-Modell is linear. The resulting normal matrices are always well-conditioned, provided that the Gaussian function or the multi-quadric are used. In this case, the polynomial structure $p(\boldsymbol{x})$ in the approximation model is dispensable. In other cases, the constraints on the distribution of points over the surface to be approximated are very mild. Thereby, the inclusion of the polynomial $p(\boldsymbol{x})$ in the approximation model is crucial. If, however, the shape-determining parameters of radial basis functions should be estimated, illconditioned equation systems are probable.

Especially in the case of TLS point clouds, the introduction of a basis function in each measurement point may lead to very large system matrices. To reduce the computational complexity, the approximation problem can be started with a small number of basic functions. Insight from the correlation length and the structure of the measurement data (see /Kauker et al. 2016/) may be included in the selection process of the centre points. Subsequent, additional basis functions are introduced sequentially in areas with high approximation residuals. Regarding the quality of the approximation, studies have shown that radial basis functions with infinite support outperform those with localization properties /Carr et al. 2001/. The latter may support the formation of artefacts.

Exemplary for this approximation method, the vertical velocity field of a crustal deformation modelled by radial basis functions is shown in *Fig. 3*. For this purpose, Gaussian functions have been used.

3 MODELLING ACTIVITIES RELATED TO THE MEASURING OBJECTS

3.1 Modelling of point clouds for the deformation analysis of bridges

Monitoring of bridges with terrestrial laser scanning is usually focused on the detection of deformations of the superstructure. In this case the superstructure is monitored from underneath with no restriction to the traffic flow (compared to the levelling). Both,

epochal and time-continuous approaches have been developed. All research activities discussed in this section are classified according to /Ohlmann-Lauber & Schäfer 2011/ in the category of geometry based models.

/Kopacik et al. 2013/ report results of epochal monitoring at several bridges over a period of up to four years. Their acquirement always follows the same methodology with its automation described in /Erdelyi 2016/. The transformation of the measurements into the same coordinate system is realized by external targets, which is essential for comparability. For the point cloud analysis, the surface of the superstructure is divided into square-shaped elements. The element size is adapted to the shape of the object. Planes are fitted to the measurements contained in an element based on modelling of quadrics described in *Section 2.1*. The geometrical information about the state of the structure for each epoch is represented by the heights of the centres of these planes. Then, the deformation is derived from height differences of these points. Its statistical significance is evaluated with respect to the scanner accuracy. In this way, the derived deformations show a discrepancy of up to 3 mm compared to the results of geometric and trigonometric levelling.

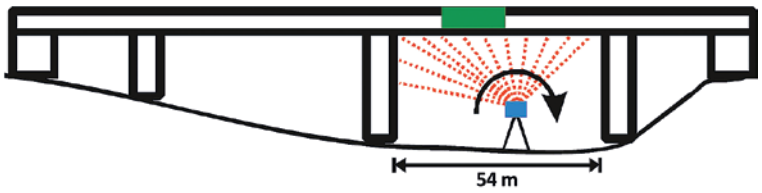

Fig. 4 | Principle of the profile measurements at bridges /Kutterer et al. 2009/

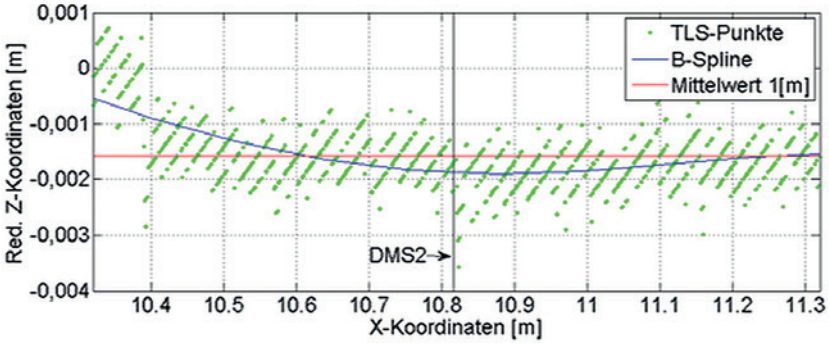

Fig. 5 | Modelling of a profile by elements with constant length (red) and by B-Spline-curves (blue) /Schmitt et al. 2013/

Continuous measurements of bridges with terrestrial laser scanning are related to the investigation of deformations caused by traffic load. Due to the high dynamics of this type of load, the scanner is operated in profile mode, which ensures repetition rates of several ten Hertz. The measured profiles are mostly oriented in longitudinal direction of the superstructure (see *Fig. 4*). Original approaches to derive deformations from profile measurements were methodologically similar to the previously described procedure for 3D point clouds: the profile is divided into elements of constant length and the height variation of their centres provides the deformation information. /Garmann et al. 2014/ enhanced this method by a space continuous modelling of profiles with Bezier and B-spline curves (see /Bureick et al. 2016/). The necessary parameter estimation of the curve integrates a sequential identification and elimination of outliers and an assessment of the approximation results by the distribution analysis of residuals. Further the cross-validation confirms the result of the approximated curves as being representative for the entire measured profile. The added value of the space-continuous modelling of the profiles compared to the elementwise approach becomes clear from *Fig. 5*, which shows the original TLS observations and their modelling by both mentioned approaches. With the space-continuous modelling, it is possible to gain a continuous representation of deformation at any point of the superstructure.

Additionally, /Neuner et al. 2014/ use the same modelling strategy of profiles to convert deformations in vertical direction into a strain signal. This is done with an artificial neural network (ANN). Its inner structure is setup based on the mechanical relationship between bending and strain for a both-side clamped beam. The training of the ANN consists of paired values of vertical displacements derived from modelled B-spline curves at the measured positions of strain gauges and their strain measurement.

3.2 Modelling of point clouds for the deformation analysis of locks

Locks are one of the first types of structures, where deformation measurements took place with terrestrial laser scanning. The activities focused mainly on the detection of the deformation of the water gates due to varying water pressure. In recent years, the number of research papers with the content of monitored locks by TLS, significantly decreased. Representative, the parameter based model of /Lindenbergh & Pfeifer 2005/ is discussed. Here, the water gate is scanned twice from the same instrument station at different water levels. Before modelling the point cloud, it is segmented into individual planes. Subsequently, the epoch-related adjustment of planes take place (see *Section 2.1*). The identity of the parameters between corresponding planes is verified by statistical tests. The location-dependent distribution of the test statistics is an expressive image of occurring deformations at the individual sub-planes of the water gate.

3.3 Modelling of point clouds for the deformation analysis of dams

The deformation analysis of dams based on levelling and total stations is a standard task in engineering geodesy. By combining both techniques in a network adjustment, two-dimensional deformations (total

station) as well as height changes (levelling) can be revealed between two epochs with up to sub-millimetre accuracy. In the recent years, laser scanners are additionally used to monitor concrete dams /Schneider 2006/. In these cases, the laser scanner serves as a supplement to the previous mentioned techniques to reveal areal deformations of the complete brickwork of the dam's downstream face. To be able to combine all techniques and to compare the measurements of different epochs, a stable registration (or geo-referencing) is needed. This is gained by permanently installed targets or other control points, respectively, on the dam structure or outside of it.

/Alba et al. 2006/ monitored the dam of Cancano Lake which is of 136 m height and of 381 m length. For analysing potential areal deformations between two epochs, they pre-processed the point clouds by resampling to a regular two-dimensional grid to get unique regularized point clouds. Afterwards, the point clouds are either meshed triangularly or they are interpolated to a regular polynomial 3D surface. The subsequent comparison of epochs is then performed in different ways: mesh to resampled point cloud, mesh to mesh, polynomial surface to resampled point cloud and polynomial surface to polynomial surface. In all cases, the shortest distance between both models is used to represent the deformation. While the first two analyses are surface based due to building a mesh of the point cloud, the latter two are geometry based due to using a polynomial representation for revealing deformations. It has to be noted, that the results vary between all strategies at a level of one sixth of the maximum deformation, detected in the middle section.

Using radial basis functions as introduced in *Section 2.2*, /González-Aguilera et al. 2008/ analysed the areal deformations of the Las Cogotas concrete dam which is of 66 m height and of 300 m length. The radial basis functions are used to build parametric 3D surfaces. To weaken the impact of data gaps and gross errors, a robust estimator is used for parameter estimation. Afterwards, these 3D surfaces are cut to multiple orthogonal cross sections (horizontal and vertical) that are compared between different epochs. *Fig. 6* shows the deformations for a horizontal cross section. This approach is – due to the approximation by radial basis functions – geometry based.

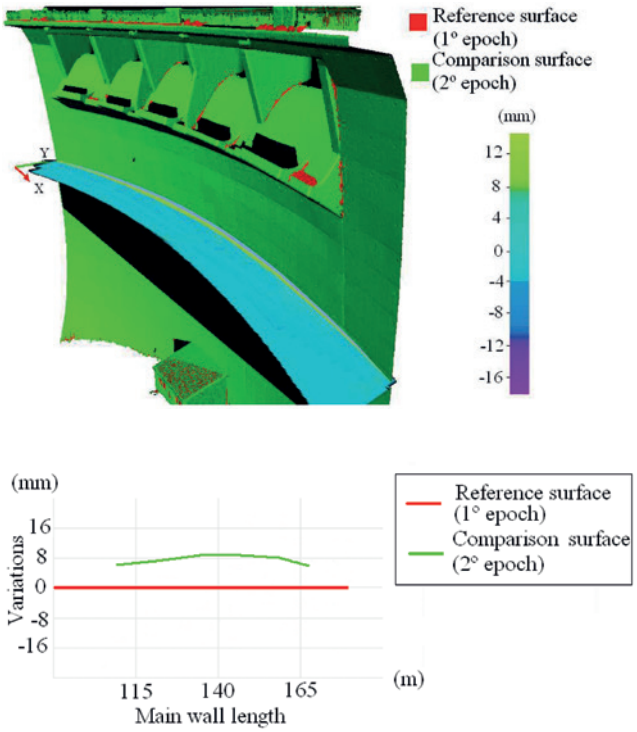

Fig. 6 | Horizontal cross section of the deformation of the Las Cogotas dam /González-Aguilera et al. 2008/

The Oker dam of 260 m length and 74 m height has been monitored by /Eling 2009/ and /Eling & Kutterer 2007/. The general structure of this dam can be parameterized by a quadric, i. e., an ellipsoid, which has already been shown in *Fig. 1*. To be able to compare the shapes acquired in two epochs, mathematically defined blocks are built. Here, each point is assigned to one block and all points inside each block are afterwards reduced to one representative point by approximating all points inside the blocks by individual planes. The difference between the representative points of corresponding blocks between two epochs is finally the measure for analysing the deformation.

The deformation of the dam is, thus, analysed for each block individually. Consequently, this approach reduces the laser scanner point clouds of several millions of points to fewer representative block points that can be assumed to be identical between two epochs. Therefore, it presents the transition of the area-based sampling of a laser scanner to the well-known analysis of discrete, identical points. Since the approximation of local planes to the point cloud is the basis of this analysis, this approach can be grouped into the category of geometry based methods. At the same time this model could also be seen as point cloud based since two point clouds of "identical" points are compared.

3.4 Modelling of point clouds for the deformation analysis of towers

Towers, e. g., cooling towers and television towers, and tower-like buildings, e. g., bridge pylons, usually consist of a relatively small ground area but of a relatively large height. Hence, most times laser scanner based deformations analyses of these buildings aim at describing deviations that vary with the height. Since these buildings are man-made structures, they are based on a mathematical model which can be described by geometrical parameters. Hence, the point cloud acquired by a laser scanner is usually modelled geometry based or parameter based for revealing the deformations.

/Pesci et al. 2015/ use a laser scanner to analyse the areal deformations of the historical 97 m high Asinelli tower, Bologna, Italy, that occurred during a seismic sequence. The tower was built 900 years ago. It has a square cross section and consists partially of selenite blocks, partially of brick-faced rubble core masonry and partially of solid-brick masonry structure. Due to this changing structure and several forces deforming the tower over 900 years, it cannot be modelled by a quadric based on only few parameters as depicted in (*1*).

By approximating a plane to each of the four towers parts separately, the planes' inclinations as well as local deviations of the point cloud from these planes can be analysed. Since the point cloud is modelled based on geometric primitives in this case and since the orientation of these primitives is of relevance, deformations are analysed geometry based. It is revealed that the tower is inclined leading to deviations of several ten centimetres at its top. Furthermore, by analysing the RMS of a moving plane along the towers height, a structural discontinuity at about 2/3 of the tower height is detected after the seismic sequence.

For the deformation analysis of a cooling tower, /Ioannidis et al. 2006/ perform a two-step geometry based deformation analysis. At first, they model the point cloud based on free-form surfaces, i. e., non-uniform rational B-Splines (NURBS). This step reduces the laser scanners' noise. In the second step, this model is compared to a quadric, as shown in (*1*), gained out of the point cloud. Here, the cooling tower equals a circular hyperboloid of one sheet (see *Tab. 1*). The deviations between quadric and NURBS model imply the areal deformations of the cooling tower compared to its theoretical construction.

/Kopácik et al. 2013/ monitor the deformations of the Liberty Bridge structure, being part of a cycling route between Bratislava (Slovak Republic) and Schlosshof (Austria). Parts of this structure are the tower-like bridge pylons. To analyse their vertical displacement, horizontal intersections of 0.2 m thickness are extracted. By projecting these intersections into one layer, the three-dimensional point cloud is reduced to several two-dimensional intersections. These are approximated by a least-squares ellipse fit to analyse the displacement of the ellipses' centres with varying height to get a bending line. These ellipses are two-dimensional quadrics similar to ellipsoids in three-dimensional space (see *Tab. 1*). After building five intersections of each pylon, the bending line reveals vertical displacements of few ten millimetres. Since a geometric model is used and the corresponding parameters are analysed for revealing the deformations, this model is rather parameter based than geometry based, although the parameters' significance is not proven.

The procedure of /Kopácik et al. 2013/ is very similar to the one of /Schneider 2006/: To analyse the areal deformations of a television tower regarding a vertical displacement, the tower is scanned and afterwards the scan is reduced to several horizontal intersections at different heights. For approximation, the model of a two-dimensional circle is used, which is, again, a quadric in two-dimensional space, i. e., an ellipse with identical semi-axes. The bending line based on the circles' centres implies a vertical displacement. Again, this model is parameter based disregarding the parameters' significance test.

3.5 Modelling of point clouds for the deformation analysis of tunnels

The aims of using TLS in tunnel-monitoring are the assessment of the shape of finished tunnel-sections to determine deviations from a planned form, the investigation of several tunnel-profiles on geometric changes due to varying pressure loads – this is the common task – as well as the examination of the heading face. These three fields of activity are incorporated in the following works.

/Gosliga et al. 2006/ are considering the deviation of the observed tunnel from the planned form of a cylinder on the one hand and the deformations occurring between two epochs on the other. In the first aspect the modelling follows the approach of *Section 2.1*, in which the cylinder equations are set up directly and the specific identification of the shape is not carried out. The limitation on estimating the measurement residuals in radial direction enables a strong dimension reduction in the least-squares adjustment and distinguishes this approach. The evaluation of the deformation is done by means of the residuals of the least-squares adjustment, whereby this approach is assigned to the geometry based models. The foundation of the epoch-based comparison is a fixed grid, which is defined on the theoretical form of the tunnel. The radii of the cylindrical coordinates of all points of the same epoch lying within one grid-element are averaged. The deformations are the differences of these grid-based mean values. Because no geometric modelling precedes the grid definition, this approach is assigned to the surface based models, although there is a significance proof of the deformations with a statistical test.

The initial point of the method from /Chmelina et al. 2012/ is also the modelling of the tunnel as a cylinder. The cylinder is used as basis for the definition of an irregular grid, whereby the grid elements are not undergoing any modelling. The deformation-information results from the investigation of several grid elements which contain the measured points. The several corresponding grid elements of two epochs are aligned using the ICP-algorithm. Thus, this procedure is principally assigned to the point cloud based models, as well as to the geometry based models.

Another geometry model for TLS-convergence measurements in the tunnel is depicted by /Delaloye 2012/ and /Walton et al. 2014/. Their approach uses as a starting point the division of the point cloud into several sections along the tunnels' longitudinal direction. Initially, section lengths of 1 m are chosen. The adjustment of corresponding sections from two epochs is carried out with ICP. Afterwards the section length will be decreased sequentially and a new ICP-based alignment is carried out. This procedure will be iterated until the section lengths correspond to the measurement noise of the scanner. The outcomes of this procedure are corresponding cross sections in the point clouds of two epochs. A best fit ellipse approximates the points of a cross section. Two methods for this approximation are presented and compared to each other: the algebraic one, which is based on the contents of *Section 2.1* – adapted for curves –, and the geometric one, which minimizes the distances in radial direction by using genetic algorithms. The authors highlight the assets of the algebraic method. The deformation information is retrieved from the differences between corresponding, best adapted ellipses and contains the calculation of the radial displacement profile. It depicts the differences, which are exaggerated with a scale factor γ.

In addition to the deformations of the tunnel's intrados, whose quantification is the aim of all mentioned contributions until now, /Ohlmann-Bartusel 2008/ considers the deformations of the heading face (*Fig. 7*) for tunnels, which are built according to the New Austrian Tunnelling Method (NATM). Due to the irregular surface, a surface based model is developed, which distinguishes by several components. Before interpolating on the nodes of the fixed grid, a

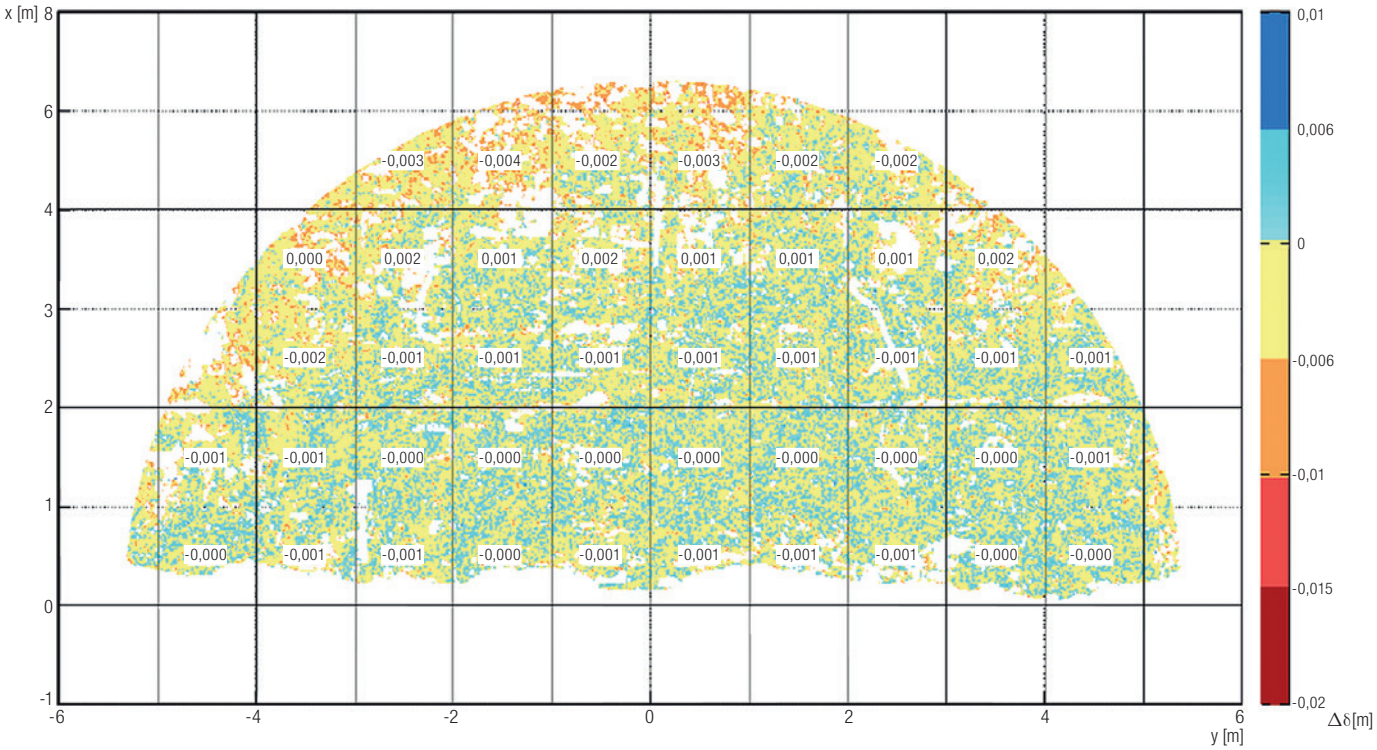

Fig. 7 | Deformations of a tunnel's heading face /Ohlmann-Bartusel 2008/

data sampling is performed. By doing this, one gets an approximately uniform distribution of the measuring points on the scanned surface. This prevents stronger weighting of measurements in areas with higher resolution in the interpolation. By using a binomial filter, a noise suppressive effect can be achieved, if it will be applied to the interpolated grid nodes. This low-pass filter causes a reduction of the noise by a factor of two to three. The third component is an adaptive filter method, which serves as an automatic elimination of pseudo-deformations. The latter are artificially induced changes of the surface, for example new layers of shotcrete or material removal. Additionally to the developed model, the outlook of this work also contains the geometric modelling with free-form surfaces (NURBS). In this case the deformations are quantified as the shortest distance to the free-form surface. These concepts are further developed by /Braun 2011/ by means of a test object.

3.6 Modelling of point clouds for the deformation analysis of geoscientific objects

In contrast to the most treated technical objects, geoscientific ones like slopes typically have a roughly unstructured surface. Therefore, predominantly point based and surface based models are used to derive deformation information from repeated laser scans. In /Barnhart & Crosby 2013/ two surface based models of the deformation of a headwall of a retrogressive thaw slump are compared: the cloud to mesh (C2M) comparison and the Multiscale Model to Model Cloud Comparison (M3C2). The C2M comprises in a first step the generation of a mesh, based on the point cloud of the reference surface. In a second step, for every point of the subsequent point cloud the distance to the nearest vertex of the generated mesh is computed. This distance is stored as deformation attribute to the respective point of the subsequent point cloud. The M3C2 algorithm also contains two steps: local point normal generation and difference estimation. In the first step, for every point of the point cloud a plane is fitted to the points in its vicinity, which is defined by a user-specified radius R. The normal vector is allocated to the considered point. Following, a cylinder with the axis aligned to the allocated normal vector and with the radius r is projected towards the subsequent point cloud. All points of the original and of the subsequent point cloud, that fall inside the cylinder are respectively averaged. The difference between the two averages is stored as deformation attribute of the considered point. The authors found that the M3C2 algorithm is more robust than C2M. This is mainly due to the integration of a spatially variable detection threshold for deformations, which results from the roughness-dependent distribution of the points inside each cylinder.

Among other relevant tasks for TLS-based deformation monitoring, like an intensity-based approach for viewpoint planning, /Wujanz 2016/ develops in his work two algorithms for the detection of stable areas in two consecutive point clouds. Common to both algorithms is a segmentation of the region of interest by means of octrees, which supports an assignment to the surface based model category. In a second step, correspondences between points are established by applying the ICP algorithm at the level of every octree cell. In the DefoScan++ algorithm the change of distances calculated between corresponding points is assessed as a basis for the decision whether a region of the octree cell is regarded as stable or deformed. The ICProx algorithm uses as a basis for comparison the span between the centres of gravity of the octree

cells in the reference and in the transformed point cloud, whereas the transformation parameters are the ones resulting from the ICP in the regarded cell. A second step of the algorithm is a congruency analysis performed in analogy to the maximum subsample method. After the detection of stable areas, the author extends the C2M method to provide a statistically justified evidence of occurred deformations. The developed algorithms are tested and evaluated among other objects at a rock glacier and an ice glacier located in the Austrian Alps.

3.7 Modelling of point clouds for the deformation analysis of special objects

Apart from the object types described so far, other objects are also analysed regarding areal deformations. These objects are noted as special, since the use of laser scanners and the areal analysis regarding deformations are rather individual cases up to now.

The main reflector of a radio telescope is such an example. It deforms during vertical rotation due to gravity. /Sarti et al. 2009/, /Dutescu et al. 2009/, /Holst et al. /2014/ and /Holst 2015/ analyse this deformation by parameterising the main reflector as a quadric, i. e., a rotational elliptic paraboloid (see *Tab. 1*). The focal length of this rotational paraboloid is the only form parameter. Hence, its elevation dependent variation describes the deformation of the reflector completely if its shape deforms homologous. Additionally, the residuals from approximation imply further local deformations from the shape. Since the estimated parameters as well as residuals from the estimated form are used for deformation analysis, the model is geometry as well as parameter based.

/Geist et al. 2016/ use radial basis functions (see *Section 2.2*) for analysing shape deformations of several parts of a yacht. The deformations are revealed by comparing the approximated surface to a reference shape. Thus, the corresponding model is geometry based. Using a ship's screw, they show the applicability of radial basis functions compared to other parameterizations, as approximation of local surfaces or moving least squares. The latter is a method for approximating continuous functions from discrete points by minimizing a weighted least squares measure, where the weights are (similar to the radial basis functions discussed in *Section 2.2*) functions of the evaluation point $\boldsymbol{x}$ and the given points $\boldsymbol{x}_i$. It is extensively described in /Levin 1998/. The comparison favours radial basis functions over the other parameterizations for detecting local shape deformations of complex large-scale structures as yachts.

/Gordon & Lichti 2007/ show the applicability of analysing the deflection of a concrete beam and a timber beam using a laser scanner. Therefore, they built up a differential equation leading to a polynomial model parameterizing the beam deflection dependent on different load scenarios. The estimated parameters define the magnitude of deformation, which is also assured by a parameter significance test. Hence, they use a parameter based model for deformation analysis showing that the vertical deflection increases with the load. /Lahamy et al. 2015, 2016/ use B-Spline curves instead for analysing the deformations based on a Microsoft Kinect 2.0. /Han et al. 2010/ use in their surface based model the deviations of a fixed mesh's centre points in the direction of measuring as deformation measure to describe the bi-axial bending of reinforced concrete slabs during static loading tests.

The deformations of single components of a car resulting from an accident are analysed by /Wujanz et al. 2016/. They use the algorithm for local surface matching ICProx, which has already been explained for the geoscientific objects (see *Section 3.6*): It is based on building local surface patches whose transformations between two epochs imply the existence of local deformations. This proceeding is surface based.

/Vezocnik et al. 2009/ use a laser scanner to determine small changes of pillars' axes positions of an underground gas pipeline. The pillars are parameterized by a quadric, i. e., a cylinder, corresponding to *Tab 1*. By estimating the cylinder axis in two epochs and by projecting this axis onto a representative point, rotational deformations of the pillars as well as translational deformations can be detected. Thus, a complete rigid body transformation is retrieved. Since the analysis of the deformation is in the end based on estimated parameters (axis of pillar), this deformation analysis is parameter based.

While all special objects are man-made structures so far, leafs of plant have also been analysed regarding areal deformations by /Dupuis et al. 2016/. These deformations are due to drought stress or general growth in this case. Therefore, the scanned leafs are meshed by a Delaunay triangulation. The deformation analysis of each leaf between two epochs is then based on counting the increase of the area of the leaf's mesh. This approach is surface based since only a mesh is used for parameterizing the leaf.

4 Summary

The contents of the previous sections are subsumed in *Tab. 3*, which reflects the applied model type and the geometric elements used for modelling the deformation of a certain object type. As can be seen, for modelling point clouds of technical objects mainly geometric and parametric models are used, whereas the modelling for geoscientific objects relies mainly on surface based models. This can be explained by the fact that surfaces of technical objects are predominantly planned using regular geometric elements. On the other hand, the surface of geoscientific objects is per se unstructured due to natural processes affecting its shape. Further, it can be asserted that among the geometric and parametric models quadrics are the most often applied method for point cloud modelling. The column statistical test indicates whether the obtained deformation is assessed statistically by means of tests. An entry in brackets reads that a statistical assessment was indicated in the study, but the test was not treated explicitly. Supplementary to the characteristics summarised in *Tab. 3*, other aspects of the approaches like the sensitivity, the robustness and the complexity are of major interest. However, the discussed papers barely address these topics and therefore, only a subjective categorisation would be possible at this stage.

A main conclusion of this study is that there is no established method for modelling point clouds, generally used in the engineering geodesy community. In fact, some researchers proofed the applicability of their developed methods to different object types but their methods were not picked-up by a large number of engineering geodesists for their applications. Furthermore, also the strategy for

	Modell type	Geometric element used for modelling	Deformation measure	Stat. Test	Monitored object component	Literature reference
Bridge	Geometry based	Free-form curves – B-Spline and Bezier	Time series	Y	Superstructure	15
	Geometry based	Free-form curves – B-Spline and Bezier	Strain	N	Superstructure	35
	Geometry based	Plane	Diff. of distances to a fixed plane	Y	Superstructure (Patches)	14, 27
Lock	Parameter based	Planes	Test results of estimated parameters of the planes	Y	Segmented parts of the lock gate	34
Dam	Geometry based	Radial basis functions	Distance between horizontal or vertical cutting curves	N	Dam – airside	16
	Geometry based	Quadric (Ellipsoid)	Distance between mesh points	Y	Dam – airside	12, 13
	Surface based Geometry based	Polynomial surface	Shortest distance between modelled elements	N	Dam – airside	1
Tower / Pylon	Geometry based	Quadric (Hyperboloid of one sheet) NURBS-Surface	Deviation to planned shape	N	Complete tower	25
	Parameter based	Circles resulting from cutting planes	Bending line	N	Complete tower	41
	Geometry based	Plane	Tilt of a sliding plane and RMS of residuals	N	Separate analysis of each side	38
	Parameter based	Ellipses resulting from cutting planes	Bending line	N	Complete tower	27
Tunnel	Surface based	Quadric (Cylinder)	Variation of mesh points in radial direction	Y	Complete tunnel tube	19
	Geometry based	Shape of cross section – Ellipse	Difference of ellipses	N	Cross profile	8, 44
	Geometry based	Quadric (Cylinder)	Transformation parameters of patches	N	Complete tunnel tube	7
	Surface based and Geometry based	Mesh and NURBS-surface respectively	Distance of points to modelled surface	Y	Heading face and adjacent tunnel section	36
Geo-scientfic objects	Surface based	Mesh	Distance between mesh points	Y	Headwall of a retro-gressive thaw slump	2
	Surface based	Octree, Mesh	Distance between mesh points	Y	Landslide	46
S1: Tele-scope	Parameter based Geometry based	Quadric (Paraboloid)	Focal length, residuals from approximation	N	Main reflector	11, 22, 23, 39
S2: Ship	Geometry based	Radial basis functions	Deviation to planned shape	N	Screw	18
S3: Beam and slab	Parameter based Surface based	Polynomials – motivated by bending lines B-Spline-Curves Mesh	Bending line Distance between mesh points	Y (17)	Complete object	17, 31, 32 20
S4: Car	Surface based	Mesh	Distance between mesh points	Y	Different car components	45
S5: Gas pipe	Parameter based	Quadric (Cylinder)	Displacement of cylinder axes	(Y)	Pillars above the gas pipe	43
S6: Plants	Surface based	Mesh	Variation of the leaf's area	(Y)	Leaf	10

S: special object type

Tab. 3 | Overview on applied model types and geometric elements in relation to types of measuring objects

pre-processing of the point clouds varies in almost every research. Different to the point based deformation analysis, where the congruency approach or the Kalman Filtering are accepted and well-established methods, this is not the case for space-continuous monitoring tasks based on point clouds. A possible strategy towards a broad acceptance of certain modelling methods could be the elaboration of free available and well-documented test data, which facilitate the comparison of already developed und published approaches. In such a case also very important aspects that remained unspecified until now, like appropriate pre-processing steps, robustness, sensitivity and complexity could be evaluated and compared. The development of methods with similar acceptance degree as in the point based case is a main research challenge for the next decade.

References

[1] Alba, M.; Fregonese, L.; Prandi, F.; Scaioni, M.; Valgoi, P. (2006): Structural Monitoring of a large Dam by Terrestrial Lasers Scanning. IAPRS, Vol. XXXVI, Part 5.

[2] Barnhart, T. B.; Crosby, B. T. (2013): Comparing Two Methods of Surface Change Detection on an Evolving Thermokarst Using High-Temporal-Frequency Terrestrial Laser Scanning, Selawik River, Alaska. In: Remote Sensing, (2013)5, 2813–2837.

[3] Braun, M. (2011): Untersuchung zur Ableitung von Deformationen aus TLS-Daten mittels Freiformflächen. Abschlussarbeit, Lehrstuhl für Geodäsie, TU München.

[4] Bronstein, I.; Semendjajew, K.; Musiol, G.; Mühlig, H. (2001): Taschenbuch der Mathematik. 5. Auflage. Harri Deutsch, Frankfurt.

[5] Bureick, J.; Neuner, H.; Harmening, C.; Neumann, I. (2016): Curve- and surface-approximation of 3D-point clouds. In: allgemeine vermessungs-nachrichten (avn), 123(2016)11-12, 315–327.

[6] Carr, J.; Beatson, R.; Cherrie, J.; Mitchell, T.; Fright, W.; McCallum, B.; Evans, T. (2001): Reconstruction and Representation of 3D Objects with Radial Basis Functions. In: Proceedings of the 28th annual conference on Computer graphics and interactive techniques. ACM, New York, NY, 67–76.

[7] Chmelina, K.; Jansa, J.; Hesina, G.; Traxler, Ch. (2012): A 3-d laser scanning system and scan data processing method for the monitoring of tunnel deformations. In: Journal of Applied Geodesy, 6(2012)3-4, 177–185.

[8] Delaloye, D. (2012): Development of a New Methodology for Measuring Deformation in Tunnels and Shafts with Terrestrial Laser Scanning (LIDAR) using Elliptical Fitting Algorithms. Thesis, Queen's University, Kingston, Ontario, Canada.

[9] Drixler, E. (1993): Analyse der Form und Lage von Objekten im Raum. Deutsche Geodätische Kommission, Reihe C, 409. Munich.

[10] Dupuis, J.; Holst, C.; Kuhlmann, H. (2016): Laser Scanner Based Growth Analysis of Plants as a New Challenge for Deformation Monitoring. In: Journal of Applied Geodesy, 10(2016)1, 37–44.

[11] Dutescu, E.; Heunecke, O.; Krack, K. (2009): Formbestimmung bei Radioteleskopen mittels Terrestrischem Laserscanning. In: Allgemeine Vermessungs-Nachrichten (AVN), 116(2009)6, 239–245.

[12] Eling, D. (2009): Terrestrisches Laserscanning für die Bauwerksüberwachung. Deutsche Geodätische Kommission, Reihe C, 641. Munich.

[13] Eling, D.; Kutterer, H. (2007): Terrestrisches Laserscanning für die Bauwerksüberwachung am Beispiel einer Talsperre. In: Brunner, F. K. (Ed.): Ingenieurvermessung 07. Beiträge zum 15. Internationalen Ingenieurvermessungskurs, Graz. Wichmann, Berlin/Offenbach, 119–130.

[14] Erdélyi, J.; Kopáčik, A.; Lipták, I.; Kyrinovič, P. (2016): Automated Point Cloud Processing to Increase the Accuracy of Deformation Monitoring. Proceedings of the 3rd Joint International Symposium on Deformation Monitoring, March 30–April 01, 2016, Vienna, Italy.

[15] Garmann, M.; Alkhatib, H.; Schmitt, C.; Neumann, I. (2014): Monitoring von Brückenbauwerken mittels Modellierung von Freiformkurven für Laserscanning-Profile. In: Luhmann Th.; Müller, Chr. (Eds.): Photogrammetrie – Laserscanning – Optische 3D-Messtechnik. Beiträge der Oldenburger 3D-Tage 2014. Wichmann, Berlin/Offenbach, 306–316.

[16] González-Aguilera, D.; Gómez-Lahoz, J.; Sánchez, J. (2008): A New Approach for Structural Monitoring of Large Dams with a Three-Dimensional Laser Scanner. In: Sensors, 8(2008)9, 5866–5883. DOI:10.3390/s8095866.

[17] Gordon, S. J.; Lichti, D. D. (2007): Modelling terrestrial laser scanner data for precise structural deformation measurement. In: Journal of Surveying Engineering, 133(2007)2, 72–80.

[18] Geist, M.; Meister, M.; Knaack, L.; Gierschner, F. (2016): Lokale Modellierung zur Bestimmung von Flächenformabweichungen mittels terrestrischer Laserscanner. In: allgemeine vermessungs-nachrichten (avn), 123(2016)3, 75–83.

[19] Gosliga, van R.; Lindenbergh, R.; Pfeifer, N. (2006): Deformation analysis of a bored tunnel by means of terrestrial laser scanning. Proceedings of the ASPRS Archives, Dresden.

[20] Han, D.; Heunecke, O.; Keuser, M.; Liebl, W.; Neumann, I.; Nichelmann, K. (2010): Anwendung des TLS zur Untersuchung des Last-Verformungsverhaltens von Flächentragwerken aus Stahlbeton. In: Wunderlich, T. (Ed.): Ingenieurvermessung 10. Beiträge zum 16. Internationalen Ingenieurvermessungskurs, München, 2010. Wichmann, Berlin/Offenbach, 57–65.

[21] Hesse, C.; Kutterer, H. (2006): Automated form recognition of laser scanned deformable objects. In: Sansò, F.; Gil, A. J. (Eds.): Geodetic deformation monitoring: from geophysical to engineering roles. In: IAG Symposia, 131. Springer, Berlin/Heidelberg/New York, 103–111.

[22] Holst, C.; Nothnagel, A.; Blome, M.; Becker, P.; Eichborn, M.; Kuhlmann, H. (2014): Improved area-based deformation analysis of a radio telescope's main reflector based on terrestrial laser scanning. In: Journal of Applied Geodesy, 9(2014)1, 1–13.

[23] Holst, C. (2015): Analyse der Konfiguration bei der Approximation ungleichmäßig abgetasteter Oberflächen auf Basis von Nivellements und terrestrischen Laserscans. Deutsche Geodätische Kommission, Reihe C, 760. Munich.

[24] IKÜS (2008): Abschlussbericht „Aufbau eines integrierten Höhenüberwachungssystems in Küstenregionen durch Kombination höhenrelevanter Sensorik (IKÜS). Geodätisches Institut, Technische Universität Dresden).

[25] Ioannidis, C.; Valani, A.; Georgopoulos, A.; Tsiligiris, E. (2006): 3D Model Generation for Deformation Analysis using Laser Scanning Data of a Cooling Tower. Proceedings of the 3rd IAG/12th FIG Symposium, May 22–24, 2006, Baden, Austria.

[26] Kauker, S.; Holst, Ch.; Schwieger, V.; Kuhlmann, H.; Schön, S. (2016): Spatio-Temporal Correlations of Terrestrial Laser Scanning. In: allgemeine vermessungs-nachrichten (avn), 123(2016)6, 170–182.

[27] Kopáčik, A.; Erdélyi, J.; Lipták, I.; Kyrinovič, P. (2013): Deformation Monitoring of Bridge Structures Using TLS. Proceedings of the 2nd Joint International Symposium on Deformation Monitoring, September 9–10, 2013, Nottingham, UK.

[28] Kuhlmann, H.; Schwieger, V.; Wieser, A.; Niemeier, W. (2014): Engineering Geodesy – Definition and Core Competencies. In: Journal of Applied Geodesy, 8(2014)4, 327–333.

[29] Kutterer, H.; Paffenholz, J.-A.; Neuner, H. (2009): Deformationsmessungen an Bauwerken mit kinematischem Laserscanning. In: Linke, H. J. (Ed.): Tagungsband zum 1. Darmstädter Ingenieurkongress – Bau und Umwelt, September 14–15, 2009, Darmstadt, Germany. CD-ROM.

[30] Kutterer, H.; Schön, S. (1999): Statistische Analyse quadratischer Formen – der Determinantenansatz. In Allgemeine Vermessungs-Nachrichten (AVN), 106(1999)10, 322–330.

[31] Lahamy, H.; Lichti, D.; Steward, J.; El-Badry, M.; Moravvej, M. (2016): Measurement of Deflection in Concrete Beams during Fatigue Loading Test using the Microsoft Kinect 2.0. Proceedings of the 3rd Joint International Symposium on Deformation Monitoring, March 30–April 01, 2016, Vienna, Austria.

[32] Lahamy, H.; Lichti, D.; El-Badry, M.; Qi, X.; Detchev, I.; Steward, J.; Moravvej, M. (2015): Evaluating the capability of time-of-flight cameras for accurately imaging a cyclically loaded beam. In: Videometrics, Range Imaging and Applications XIII, Munich, Germany, 95280V-1–95280V-11.

[33] Levin, D. (1998): The approximation power of moving least-squares. In: Mathematics of computation, 67(1998)224, 1517–1531.

[34] Lindenbergh, R.; Pfeifer, N. (2005): A statistical deformation analysis of two epochs of terrestrial laser data of a lock. In: Proceedings of the 7th Conference on Optical 3-D Measurement Techniques, October 3-5, 2005, Vienna, Austria, 61–70.

[35] Neuner, H.; Schmitt, C.; Neumann, I. (2014): Zur Bestimmung der verkehrsseitig verursachten Dehnung an einem Brückentragwerk mittels terrestrischem Laserscanning. In: Wieser, A. (Ed.): Ingenieurvermessung 14. Beiträge zum 17. Internationalen Ingenieurvermessungskurs Zürich, 2014. Wichmann, Berlin/Offenbach, 231–243.

[36] Ohlmann-Bartusel, J. (2008): Innovative determination of areal deformations of an excavated tunnel intrados by multi-temporal laser scanning data – Potential of driving-attendant tunnel scanning for the NATM. Diploma Thesis, Chair of Geodesy, Institute of Geodesy, GIS and Land Management, Technische Universität München (unpublished).

[37] Ohlmann-Lauber, J.; Schäfer, T. (2011): Ansätze zur Ableitung von Deformationen aus TLS-Daten. In: 106. DVW-Seminar Terrestrisches Laserscanning – TLS 2011, Wißner, Augsburg, 161–180.

[38] Pesci, A.; Teza, G.; Boschi, E. (2015): Laser scanning-based detection of morphological changes of a historical building occurred during a seismic sequence: Method and Case study. In: International Journal of Geomatics and Geosciences, 5(2015)3, 427– 447.

[39] Sarti, P.; Vittuari, L.; Abbondanza, C. (2009): Laser scanner and terrestrial surveying applied to gravitational deformation monitoring of large VLBI telescopes' primary reflector. In: Journal of Surveying Engineering, 135(2009)4, 136–148.

[40] Schmitt, C.; Neuner, H.; Neumann, I.; von der Haar, C.; Hansen, M.; Marx, S. (2013): Überwachung von Brückentragwerken mit ingenieurgeodätischen Verfahren und Sensoren der Baumesstechnik. In: Sörgel, U.; Schack, L. (Eds.): Tagungsband Geomonitoring 2013, March 15–16, 2013, Hannover, Germany, 81–103.

[41] Schneider, D. (2006): Terrestrial Laser Scanning for Area Based Deformation Analysis of Towers and Water Dams. Proceedings of the 3rd IAG/12th FIG Symposium, May 22–24, 2006, Baden, Austria.

[42] Schön, S.; Kutterer, H. (1999): Analyse statistique des formes quadratiques la méthode des déterminants. In: Association Francaise de Topographie, XYZ, 21(1999), 70–75.

[43] Vezočnik, R.; Ambrožič, T.; Sterle, O.; Bilban, G.; Pfeifer, N.; Stopar, B. (2009): Use of Terrestrial Laser Scanning Technology for Long Term High Precision Deformation Monitoring. In: Sensors, 9(2009)12, 9873–9895.

[44] Walton, G.; Delaloye, D.; Diederichs, M. S. (2014): Development of an elliptical fitting algorithm to improve change detection capabilities with applications for deformation monitoring in circular tunnels and shafts. In: Tunneling and Underground Space Technology, 43(2014), 336–349.

[45] Wujanz, D.; Krueger, D.; Neitzel, F. (2016): Identification of stable areas in unreferenced laser scans for deformation measurement. In: The Photogrammetric Record, 31 (2016)155, 261–280.

[46] Wujanz, D. (2016): Terrestrial Laser Scanning for Geodetic Deformation Monitoring. Dissertation, TU Berlin.

[47] Wunderlich, Th.; Niemeier, W.; Wujanz, D.; Holst, Ch.; Neitzel, F.; Kuhlmann, H. (2016): Areal Deformation Analysis from TLS Point Clouds – the Challenge. In: allgemeine vermessungs-nachrichten (avn), 123(2016)11-12, 340–351.

Prof. Dr.-Ing. Hans Neuner

TU WIEN
DEPARTMENT OF GEODESY
AND GEOINFORMATION

Gußhausstraße 27–29 | A-1040 Wien
hans.neuner@geo.tuwien.ac.at

Dr.-Ing. Christoph Holst

UNIVERSITÄT BONN
INSTITUT FÜR GEODÄSIE
UND GEOINFORMATION (IGG)

Nußallee 17 | 53115 Bonn
c.holst@igg.uni-bonn.de

Prof. Dr.-Ing. Heiner Kuhlmann

UNIVERSITÄT BONN
INSTITUT FÜR GEODÄSIE
UND GEOINFORMATION (IGG)

Nußallee 17 | 53115 Bonn
heiner.kuhlmann@uni-bonn.de

Manuskript eingereicht: 13.09.2016 | Im Peer-Review-Verfahren begutachtet